When Design Rules Break: Benchmark Composition Determines Whether Label Informativeness Predicts GNN Aggregator Choice

Neha Sharma *sharman20@vcu.edu*
Department of Computer Science
Virginia Commonwealth University

Ritesh Sharma *sharmar33@vcu.edu*
Department of Electrical and Computer Engineering
Virginia Commonwealth University

Abstract

A design rule that holds within one graph family may fail on another that legacy benchmarks do not cover. We demonstrate this through a controlled ablation of aggregator selection (sum, mean, max) across 24 node-classification datasets spanning citation, cleaned heterophilic, LINKX Facebook-100, co-purchase, and co-authorship graphs, varying only the aggregation operator. Edge homophily weakly predicts the GIN-Sum vs. GIN-Mean accuracy gap (Spearman $\rho = 0.46$). Label informativeness predicts it well on legacy benchmarks ($\rho = 0.885$, 88% LOO on 16 stable-learning datasets) but only weakly across the full suite ($\rho = 0.51$), the difference driven entirely by the LINKX Facebook-100 graphs: four dense friendship networks with near-zero informativeness favor sum aggregation by 7–10% ($p < 0.005$), rising to $\sim$13% under tenfold-extended training. Stochastic block model ablations, including a degree-corrected variant at LINKX-scale degrees, fail to reproduce this, ruling out mean degree as the trigger. Among five label-independent statistics, the spectral gap separates the LINKX graphs from every other low-LI dataset (Mann–Whitney $p = 0.002$); the effect localizes to the one-hop neighborhood and replicates under GCN and BatchNorm. The LINKX regime is thus structurally isolable but not yet a closed-form rule. We further identify three training regimes interacting with aggregator choice, and show PNA loses to the best single-aggregator GIN by 9–16% on Cora, CiteSeer, and PubMed (the high- vs. low-LI margin difference is significant at $p = 0.036$ but vanishes once these three are removed, $p = 0.446$). Our central finding is methodological: benchmark composition, not numerical insufficiency, determines whether design rules generalize; all GIN findings require separate validation before extending to other architectures, and the LINKX regime gives adaptive aggregation methods a concrete benchmark target.

1 Introduction

A widely used heuristic in graph neural network (GNN) design holds that sum aggregation is preferable for homophilous graphs, whereas mean aggregation is better suited for heterophilic regimes. This intuition appears across prior work, where aggregation choice is implicitly tied to graph statistics such as homophily or degree normalization (Xu et al., 2019; Corso et al., 2020; Luan et al., 2023). Yet these claims are typically validated on a narrow set of benchmarks. Whether such design rules generalize, however, depends critically on which benchmarks are used for evaluation — a dependence that stays hidden when benchmark suites are narrow.

We revisit this assumption from a benchmark-centric perspective. We assemble a controlled evaluation suite of 24 node-classification datasets spanning citation networks, cleaned heterophilic benchmarks (Platonov

et al., 2023), LINKX Facebook-100 graphs (Lim et al., 2021), co-purchase, and co-authorship networks, covering edge homophily $h \in [0.05, 0.93]$ and label informativeness LI $\in [0.00, 0.72]$. Every model is trained under an identical protocol; only the aggregator differs.

Our results show that the standard heuristic does not generalize uniformly. Edge homophily is only weakly predictive ($\rho = 0.46$). For GIN, label informativeness (Platonov et al., 2023) explains outcomes far better on canonical benchmarks ($\rho = 0.885$ on 16 stable-learning datasets; a single threshold rule achieves 88% LOO accuracy), but breaks down on the LINKX Facebook-100 graphs, where four dense friendship networks with near-zero informativeness consistently favor sum aggregation by 7–10% ($p < 0.005$). This advantage persists under tenfold-extended training. Two stochastic block model ablations – a homogeneous SBM up to $\bar{d} = 30$ and a degree-corrected SBM extended to LINKX-scale degrees ($\bar{d} \in \{50, 60, 70\}$) – fail to reproduce the regime: mean aggregation wins across the homogeneous grid, and the degree-corrected extension shows no degree trend ($\rho(\bar{d}, \text{gap}) = +0.14$, $p = 0.45$). Neither uniform nor heavy-tailed degree heterogeneity is the trigger. No homophily-family statistic predicts the LINKX regime, but a structural statistic outside that family – the spectral gap of the normalized Laplacian – separates it from every other low-LI dataset in our suite (Section 4.3).

More broadly, aggregator performance is governed by three distinct training regimes — stable-learning, sum-saves-it, and all-collapse — that are unevenly represented across existing benchmarks. Design rules that work well on standard datasets can therefore fail completely when evaluated on a benchmark family that occupies a previously untested region of graph-statistic space. These findings matter to two audiences: GNN practitioners who currently rely on edge homophily as an aggregator-selection heuristic, and graph-benchmark designers seeking diagnostic statistics that generalize across graph families.

Contributions. This work makes the following contributions:

1. A controlled ablation across 24 node-classification benchmarks showing that edge homophily is a weak predictor of aggregator choice (Section 4.1).

2. Evidence that label informativeness predicts GIN aggregator choice on legacy benchmark suites (88% LOO on 16 stable-learning datasets) but fails on the LINKX family, with the failure not supported by mean degree in a purpose-built SBM ablation; the structural correlate of this failure is identified separately (Contribution 4) (Sections 4.2–4.3, Appendix B).

3. A cross-architecture replication showing the LI rule does not transfer cleanly to GraphSAGE ($\rho = 0.32$, n.s.), and that disabling the self-loop pathway widens rather than closes the gap (Section 4.6, Appendix A).

4. A structural characterization of the LINKX regime: among five label-independent graph statistics, the spectral gap λ_2 is the strongest discriminator of LINKX versus all other low-LI datasets (distributionally significant at Mann–Whitney $p = 0.0022$, though not a perfectly separating threshold), the effect is localized to the one-hop neighborhood, and it replicates under GCN and strengthens under BatchNorm — elevating the LINKX regime from unexplained to structurally isolated though not yet a closed-form rule (Sections 4.3, 4.6; Appendices H, I, J, K).

5. An operational regime classification isolating the 21 datasets on which aggregator comparison is well-defined, with Roman-empire identified as a learnability outlier (Section 4.4).

6. A regime-split analysis of PNA showing it underperforms the best single-aggregator GIN by 9–16% per dataset on canonical citation benchmarks (Cora, CiteSeer, PubMed), with PNA's overall margin significantly worse on high-LI graphs than low-LI graphs (Section 4.5).

7. A methodological finding that benchmark composition — not numerical insufficiency — determines whether a design rule holds: the LI rule achieves near-perfect accuracy on legacy benchmarks yet collapses on LINKX, a regime that legacy suites never cover (Section 5).

2 Related work

Aggregation in message-passing GNNs. Kipf & Welling (2017) introduce GCN with degree-normalized mean aggregation; Veličković et al. (2018) replace fixed weights with attention; Hamilton et al. (2017) introduce GraphSAGE with selectable mean/max/LSTM aggregators. Xu et al. (2019) prove that GIN with sum aggregation is the most expressive 1-WL message-passing GNN, and provide an ablation comparing sum, mean, and max on graph classification. Our work extends this ablation to node classification across a homophily-ordered benchmark suite and asks whether graph statistics predict the aggregator choice.

Multi-aggregator architectures. Corso et al. (2020) introduce Principal Neighbourhood Aggregation (PNA), which combines mean, max, min, and standard deviation aggregation with degree scalers. PNA is the most direct prior work on aggregator-graph-structure interaction; we use it as a baseline and find it does not uniformly dominate the best single aggregator on the benchmarks we test. Other work explores learned readouts and soft attention over aggregators; we focus on the narrower question of whether fixed-aggregator preference can be predicted from graph statistics.

Selection and adaptation mechanisms. A complementary line of work proposes architectures that adapt aggregation or depth to local graph structure rather than committing to a fixed operator. Maurya et al. (2022) decouple feature generation from depth and learn a soft selector over multi-hop features, observing that the optimal hop selection differs between homophilic and heterophilic graphs. Hevapathige et al. (2026) propose adaptive per-node propagation depth tied to local homophily, addressing the same underlying observation that fixed design rules generalize poorly across graph regimes. From a theoretical angle, Ghogho (2025) reanalyzes neighborhood aggregation through statistical signal processing and argues that standard mean and sum operators can be conceptually flawed under common node-classification assumptions. These works approach the brittleness of fixed aggregation by proposing adaptive architectures, while we characterize the brittleness empirically and document a regime (LINKX Facebook-100) where no current graph statistic predicts aggregator preference — providing a concrete benchmark target for adaptive methods.

Heterophily-specialized GNN architectures. A parallel line of work designs architectures specifically for heterophilic graphs: H2GCN separates ego- and neighbor-embeddings and uses higher-order neighborhoods (Zhu et al., 2020); GPR-GNN adaptively learns propagation weights across the homophily–heterophily spectrum (Chien et al., 2021); MixHop mixes representations across powers of the adjacency matrix (Abu-El-Haija et al., 2019); ACM combines aggregation, diversification, and identity channels per node (Luan et al., 2022); and Geom-GCN is the original geometric heterophily-aware method (Pei et al., 2020). These adapt the propagation operator to graph structure. We ask the dual question: with the architecture fixed, do graph statistics predict which aggregator to use? Our LINKX results identify a regime where the answer is no.

Heterophily metrics and alternative diagnostics. Zhu et al. (2020) introduce the edge homophily ratio as a diagnostic metric and show that standard GNNs degrade on low-homophily graphs. Ma et al. (2022) qualify this picture by showing that GCN can perform well on some heterophilic graphs, particularly when within-class neighborhood distributions are distinguishable across classes, suggesting that edge homophily alone is an incomplete characterization. Beyond edge homophily, the literature has proposed several alternative diagnostics: node-level homophily (Pei et al., 2020), adjusted homophily and label informativeness (Platonov et al., 2023), generalized homophily metrics for non-homophilous graphs (Lim et al., 2021), and post-aggregation similarity metrics (Luan et al., 2022). Our work focuses on label informativeness because it is the most direct information-theoretic refinement of edge homophily and is recommended by its authors as a stronger diagnostic; however, we document a regime where no scalar diagnostic in this family suffices.

Label informativeness and benchmark critique. Platonov et al. (2023) demonstrate that the original heterophilic benchmarks (Chameleon, Squirrel, Cornell, Texas, Wisconsin) have data quality issues, contain duplicate nodes causing train-test leakage, and that edge homophily is a poor predictor of GNN accuracy on cleaned datasets. They introduce label informativeness as a stronger diagnostic and release a new benchmark suite. Our work directly extends their critique from accuracy prediction to aggregator selection: we show

that LI predicts the sum-vs.-mean gap dramatically better than edge homophily on their benchmarks, but identify a separate dataset family (LINKX (Lim et al., 2021)) where neither metric suffices.

Empirical methodology and strong baselines. A growing line of work emphasizes careful empirical evaluation in graph learning. Shchur et al. (2018) document evaluation pitfalls on standard node-classification benchmarks, including high variance across splits and inappropriate hyperparameter selection. Hu et al. (2020) introduce the Open Graph Benchmark, providing large-scale datasets with unified evaluation protocols and arguing that small-scale benchmarks (Cora, CiteSeer, PubMed) are insufficient for distinguishing modern GNN variants. Platonov et al. (2023) extend this critique to the original heterophilic benchmarks. Most recently, Luo et al. (2024) show that well-tuned GCN, GAT, and GraphSAGE match or exceed Graph Transformers on 17 of 18 node-classification benchmarks. Our results corroborate the strong-baselines view by showing classic baselines outperform GIN variants on most homophilous datasets; we treat the GIN family as a *controlled testbed* for the aggregator question rather than as a proposed best architecture, and contribute to this empirical methodology line by showing that benchmark composition itself determines whether design rules generalize.

3 Setup

3.1 Benchmarks

We evaluate on 24 node-classification benchmarks summarized in Table 1. The suite covers four loosely-grouped families: classic citation networks (Yang et al., 2016); the original heterophilic benchmarks (Pei et al., 2020; Chiang et al., 2019); the cleaned heterophilic benchmarks of Platonov et al. (2023); and the LINKX Facebook-100 social graphs (Lim et al., 2021). We additionally include Actor (Tang et al., 2009), the Amazon co-purchase networks (Shchur et al., 2018), the Coauthor academic networks (Shchur et al., 2018), and DBLP. Edge homophily h ranges from 0.05 (Roman-empire) to 0.93 (Coauthor-Physics); label informativeness LI ranges from essentially zero (Minesweeper, Actor, Penn94) to 0.72 (Coauthor-Physics).

3.2 Models and training protocol

We compare seven message-passing models: GCN (Kipf & Welling, 2017), GAT (Veličković et al., 2018), GraphSAGE-Mean (Hamilton et al., 2017), the three GIN variants GIN-Sum, GIN-Mean, GIN-Max (Xu et al., 2019), and PNA (Corso et al., 2020). The GIN variants share the MLP, depth, dropout, optimizer, and learning rate; only the aggregator differs. All three are implemented via a custom `GINConvVariant`. At layer k each variant computes

$$\mathbf{h}_v^{(k)} = \mathrm{MLP}^{(k)}\Big((1+\varepsilon^{(k)})\,\mathbf{h}_v^{(k-1)} + \mathrm{AGG}_{u\in\mathcal{N}(v)}\,\mathbf{h}_u^{(k-1)}\Big), \tag{1}$$

where $\mathcal{N}(v)$ is the set of neighbors of v *excluding* v itself (no self-loops are added to the edge index; the self-contribution enters only through the $(1+\varepsilon^{(k)})$ term), and $\varepsilon^{(k)}$ is a per-layer scalar initialized to 0 and learned during training. The three variants instantiate AGG, over the F feature dimensions, as

$$\underbrace{\sum_{u\in\mathcal{N}(v)} \mathbf{h}_u}_{\texttt{sum}}, \qquad \underbrace{\frac{1}{|\mathcal{N}(v)|}\sum_{u\in\mathcal{N}(v)} \mathbf{h}_u}_{\texttt{mean}}, \qquad \underbrace{\Big(\max_{u\in\mathcal{N}(v)} h_{u,1},\ \ldots,\ \max_{u\in\mathcal{N}(v)} h_{u,F}\Big)}_{\texttt{max}}.$$

We use no BatchNorm, LayerNorm, or residual connections in any GIN variant, so the comparison isolates aggregator effects. We note in Section 5 that this leaves a potential confound between aggregator expressivity and activation-scale dynamics on dense graphs. All models use 2 layers, hidden dimension 64, dropout rate = 0.5, Adam optimizer with learning rate 10^{-3}, weight decay 5×10^{-4}, up to 300 epochs with early stopping on validation accuracy or AUC (patience 50). For binary-task Platonov datasets (Minesweeper, Tolokers, Questions) we use AUC-driven model selection following Platonov et al. (2023).

For Cora, CiteSeer, and PubMed we use the standard public splits (Yang et al., 2016). For datasets with predefined multi-splits (WikipediaNetwork, WebKB, HeterophilousGraphDataset, Actor, LINKX), we use the

Table 1: The 24 node-classification benchmarks. h = edge homophily, LI = label informativeness (Platonov et al., 2023), $\bar{d}$ = mean degree, λ_2 = algebraic connectivity (second-smallest eigenvalue of the symmetric normalized Laplacian). For the one materially disconnected dataset, JohnsHopkins55 (11 components, 5157/5180 nodes in the largest connected component, LCC), λ_2 is computed on the LCC; all other datasets are connected or have a single dominant component covering $> 99\%$ of nodes (per-dataset component counts are released with the supplementary code). Entries shown as 0.000 are small positive values rounded to three decimals on connected (or $> 99\%$-dominant-component) graphs, not disconnection artifacts; exact values are released with the supplementary code.

Dataset	Family	Nodes	h	LI	$\bar{d}$	λ_2	Classes
Cora	Citation	2,708	0.81	0.59	3.9	0.005	7
CiteSeer	Citation	3,327	0.74	0.45	2.7	0.002	6
PubMed	Citation	19,717	0.80	0.41	4.5	0.014	3
DBLP	Citation	17,716	0.83	0.46	5.5	0.002	4
Coauthor-CS	Coauthor	18,333	0.81	0.65	8.9	0.004	15
Coauthor-Physics	Coauthor	34,493	0.93	0.72	14.4	0.016	5
Amazon-Computers	Co-purchase	13,752	0.78	0.53	35.8	0.017	10
Amazon-Photo	Co-purchase	7,650	0.83	0.67	31.1	0.003	8
Chameleon	Wikipedia	2,277	0.24	0.05	15.9	0.006	5
Squirrel	Wikipedia	5,201	0.22	0.00	41.7	0.039	5
Actor	Wikipedia	7,600	0.22	0.00	7.9	0.000	5
Cornell	WebKB	183	0.13	0.09	1.6	0.077	5
Texas	WebKB	183	0.11	0.15	1.8	0.032	5
Wisconsin	WebKB	251	0.20	0.10	2.1	0.036	5
Roman-empire	Platonov	22,662	0.05	0.11	2.9	0.000	18
Amazon-ratings	Platonov	24,492	0.38	0.04	7.6	0.000	5
Minesweeper	Platonov	10,000	0.68	0.00	8.0	0.000	2
Tolokers	Platonov	11,758	0.59	0.01	88.3	0.067	2
Questions	Platonov	48,921	0.84	0.00	6.3	0.008	2
Penn94	Facebook-100	41,554	0.51	0.00	65.4	0.155	2
Reed98	Facebook-100	962	0.52	0.00	38.0	0.178	2
Amherst41	Facebook-100	2,235	0.53	0.00	90.4	0.120	2
Cornell5	Facebook-100	18,660	0.55	0.01	80.7	0.078	2
JohnsHopkins55	Facebook-100	5,180	0.55	0.01	70.5	0.126	2

i-th of the bundled splits at seed i. For other datasets we generate a random 60/20/20 split per seed. Each (dataset, model) cell is run for 10 seeds; we report mean and standard deviation.

3.3 Hyperparameter robustness sweep

To address the concern that the gap-sign might depend on hyperparameter choice, we run a grid sweep on GIN-Sum and GIN-Mean only. The grid spans hidden dim $\in \{32, 64, 128\}$, depth $\in \{2, 3\}$, dropout $\in \{0.3, 0.5\}$, and lr $\in \{10^{-3}, 5 \times 10^{-4}\}$, totaling 24 configurations per (dataset, model) cell, with 5 seeds per cell.

3.4 Synthetic SBM validation

To complement benchmark results, we generate stochastic block model graphs at a 9×5 grid of (target homophily, mean degree) settings and train both GIN-Sum and GIN-Mean on each. This validation is designed specifically to test whether mean degree at fixed LI ≈ 0 is the mechanistic trigger for the LINKX regime (Section 4.3), isolating whether observed correlations on real data are structural or benchmark artifacts. Results from this validation are reported in Appendix B.

3.5 Statistical evaluation

Notation. Throughout this paper, ρ denotes the Spearman rank correlation coefficient between two quantities (typically between a graph statistic and an aggregator-gap value across datasets), while p denotes a two-tailed significance level (from a Wilcoxon, Spearman, Mann–Whitney, or permutation test as specified in context). The two should not be confused: ρ describes the strength of a correlation, p describes the probability of observing that correlation under a null hypothesis. For each dataset we report the per-seed paired Wilcoxon signed-rank test between GIN-Sum and GIN-Mean accuracies; these are descriptive statistics characterizing individual dataset behavior and are not used as confirmatory tests.

With 10 paired seeds, $p = 0.002$ is the floor of the test and indicates unanimous sign agreement across seeds rather than effect-size discrimination. Per-dataset p-values are uncorrected since dataset-level claims are not derived from individual tests. Aggregate claims (Spearman correlations, regime classifications, threshold rules) are tested separately with 5000-sample bootstrap confidence intervals and 5000-sample permutation null tests. We fit 1D threshold rules and 2D/3D/all-feature logistic regressions, evaluating each via leave-one-dataset-out (LOO), 5-fold, and 3-fold cross-validation. Aggregate p-values are uncorrected for the multiple tests reported in Section 4.2–4.5; replication patterns and bootstrap CIs are the primary evidence.

4 Results

4.1 Edge homophily is a weak predictor

We begin by asking whether existing design heuristics, specifically the homophily aggregator rule, generalize across our chosen diversified benchmark suite. Across all 24 datasets, the Spearman rank correlation between edge homophily and the GIN-Sum minus GIN-Mean accuracy gap is $\rho = 0.46$ ($p = 0.025$). This is statistically significant but unimpressive, and three datasets violate the implied rule starkly. Minesweeper has $h = 0.68$ (high homophily) yet GIN-Mean wins by 10.5% ($p = 0.002$). Roman-empire has $h = 0.05$ (extreme heterophily) yet GIN-Sum wins by 4.9% ($p = 0.002$). Penn94, Amherst41, Cornell5, and JohnsHopkins55 all have $h \approx 0.5$ yet GIN-Sum wins by 7–10% ($p < 0.005$ in each case).

The textbook intuition therefore holds in the aggregate but fails at exactly the cases that motivate it. We test whether a different graph statistic predicts the gap better. Table 2 reports the full per-dataset breakdown sorted by label informativeness, with each dataset's training regime annotated. Figure 1 (right) plots the gap against LI, revealing the LINKX cluster near LI = 0 with positive gaps.

We center the analysis on the GIN-Sum vs. GIN-Mean comparison because it is the contrast grounded in Xu et al. (2019)'s expressiveness result; we report GIN-Max throughout the grid and analyze it fully in Appendix G, where the sharper framing emerges that *degree-normalized (mean) aggregation underperforms* — both Sum and Max beat Mean on the LINKX family and Max tracks Sum on high-LI graphs — rather than Sum being uniquely advantaged.

4.2 Label informativeness predicts the gap on legacy benchmarks

Label informativeness $\mathrm{LI}(G) = I(y_u; y_v)/H(y_v)$ (Platonov et al., 2023), where (u, v) ranges over edges, achieves $\rho = 0.51$ (95% bootstrap CI $[0.07, 0.80]$, $p = 0.012$) across all 24 datasets, modestly improving on edge homophily. Its strength is more striking on the legacy benchmark suites. On the 19 datasets that overlap with the standard Pei–Platonov heterophilic suite (excluding LINKX), $\rho = 0.87$ with $p = 1.0 \times 10^{-6}$. On the broader set of all 16 stable-learning non-LINKX datasets, $\rho = 0.885$ (95% bootstrap CI $[0.63, 0.98]$, $p < 0.001$) and LOO accuracy is 88% (14 of 16); this conditions on excluding 5 LINKX datasets and 3 non-stable-learning datasets, of which the LINKX exclusion is the dominant effect (full-suite $\rho = 0.51$ on all 24, Section 4.1). On a post-hoc 9-dataset subset (those with paired Wilcoxon $p < 0.05$ on the per-seed Sum–Mean comparison), $\rho = 0.97$ and a threshold rule achieves 100% LOO accuracy; the 88% figure on all 16 datasets is the pre-specified estimate.[1]. Permutation $p < 0.001$. Excluding the two largest-gap datasets

[1]Replacing full-graph LI with a training-edge-only estimate preserves 89% LOO accuracy (8/9 datasets); PubMed fails because the standard 60-node split yields fewer than one expected intra-mask edge. The minimum margin between any held-out

Table 2: Per-dataset GIN-Sum vs. GIN-Mean comparison sorted by label informativeness LI. Gap is the mean GIN-Sum accuracy minus mean GIN-Mean accuracy across 10 seeds; the p column reports the per-seed paired Wilcoxon p-value (not to be confused with the Spearman rank correlation ρ used in Sections 4.1 and 4.2). Regime: S = stable-learning, SS = sum-saves-it, AC = all-collapse (Section 4.4). Wisconsin's $p = 1.000$ reflects a near-zero gap with symmetric rank structure across seeds and is consistent with the null hypothesis. Coauthor-Physics ($p = 0.139$ despite gap +0.202) reflects high within-seed variance on this dataset; the gap sign is consistent in 22 of 24 hyperparameter configurations (Section 4.2).

Dataset	h	LI	GIN-Sum	GIN-Mean	gap	p	Reg.
Minesweeper	0.68	0.00	0.724	0.829	−0.105	0.002	S
Actor	0.22	0.00	0.270	0.297	−0.027	0.037	S
Penn94	0.51	0.00	0.807	0.736	+0.071	0.002	S
Reed98	0.52	0.00	0.625	0.576	+0.050	0.051	S
Questions	0.84	0.00	0.580	0.559	+0.021	0.492	S
Squirrel	0.22	0.00	0.280	0.292	−0.012	0.770	S
Amherst41	0.53	0.00	0.775	0.683	+0.093	0.002	S
Cornell5	0.55	0.01	0.802	0.726	+0.075	0.002	S
Tolokers	0.59	0.01	0.694	0.756	−0.063	0.002	S
JohnsHopkins55	0.55	0.01	0.783	0.679	+0.103	0.002	S
Amazon-ratings	0.38	0.04	0.369	0.368	+0.001	0.080	AC
Chameleon	0.24	0.05	0.340	0.363	−0.023	0.173	S
Cornell	0.13	0.09	0.454	0.454	+0.000	—	AC
Wisconsin	0.20	0.10	0.496	0.480	+0.016	1.000*	S
Roman-empire	0.05	0.11	0.188	0.140	+0.049	0.002	SS
Texas	0.11	0.15	0.600	0.595	+0.005	0.180	S
PubMed	0.80	0.41	0.774	0.758	+0.016	0.002	S
CiteSeer	0.74	0.45	0.609	0.567	+0.042	0.066	S
DBLP	0.83	0.46	0.845	0.824	+0.022	0.006	S
Amazon-Computers	0.78	0.53	0.829	0.373	+0.456	0.002	S
Cora	0.81	0.59	0.755	0.686	+0.069	0.002	S
Coauthor-CS	0.81	0.65	0.925	0.406	+0.519	0.002	S
Amazon-Photo	0.83	0.67	0.899	0.333	+0.566	0.004	S
Coauthor-Physics	0.93	0.72	0.962	0.760	+0.202	0.139	S

(Amazon-Photo, +0.566; Coauthor-CS, +0.519) leaves $\rho = 0.929$ ($p = 0.003$, $n = 7$), confirming the LI–gap relationship is not driven by these extreme values. Edge homophily and LI as predictors are compared directly in Figure 1.

Within the legacy suites the rule appears almost deterministic. Datasets with LI ≥ 0.4 (citation networks, Coauthor, Amazon co-purchase, DBLP) are uniformly sum-wins. Datasets with LI ≤ 0.01 (Minesweeper, Tolokers, Actor) are uniformly mean-wins. Any threshold in $[0.01, 0.41]$ yields the same LOO result; the rule locates a regime boundary, not its exact position. Four of our 16 stable-learning non-LINKX datasets fall in this ambiguous zone (Chameleon, Wisconsin, Roman-empire, Texas); for any new dataset with LI in this range, the reliable approach is to run both aggregators and compare per-seed.

Hyperparameter robustness. On 7 of 8 datasets with LI ≥ 0.4, the gap sign is consistent across $\geq 92\%$ of 24 hyperparameter configurations (hidden dim, depth, dropout, lr; Section 3.3); the remaining dataset (Coauthor-Physics) is consistent in 22 of 24 configurations. Six datasets are 100% consistent. On low-LI legacy datasets the gap sign is unstable, confirming the LI ≥ 0.4 rule is a structural property rather than a single-setting artifact.

dataset's LI and the fitted threshold is 0.41, confirming no dataset sits near a decision boundary. Per-dataset LI-full vs. LI-train values are released with the supplementary code.

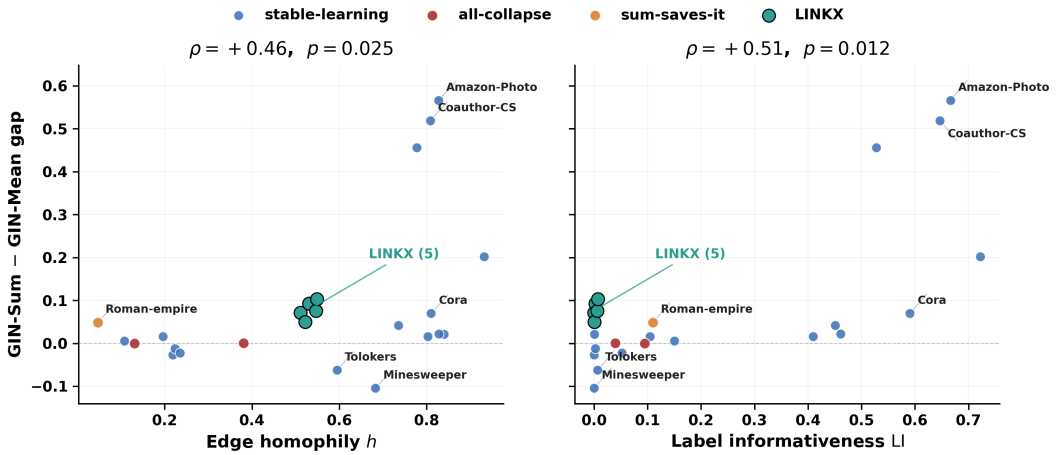

Figure 1: Edge homophily (left) versus label informativeness (right) as predictors of the GIN-Sum vs. GIN-Mean accuracy gap. Label informativeness exhibits substantially higher rank correlation with the gap on the full 24-dataset suite.

4.3 The LINKX Facebook-100 surprise

The five LINKX Facebook-100 datasets break the rule. Four of them (Penn94, Amherst41, Cornell5, JohnsHopkins55) have LI essentially zero (LI ≤ 0.007), placing them firmly on the "mean-wins" side of the fitted threshold. Yet GIN-Sum wins on every one of them by 7–10% at $p < 0.005$. Reed98 is similar in pattern but at lower significance ($p = 0.05$, gap +5.0%). Appendix G shows GIN-Max also outperforms GIN-Mean on all five LINKX datasets, so the anomaly is more precisely *degree-normalised aggregation fails* than *sum wins*; we use the latter framing throughout this section for parity with the headline GIN-Sum vs. GIN-Mean comparison.

These graphs share a feature distinct from any other low-LI dataset in our suite: they are dense friendship networks with median degree 48–70, the highest in our benchmark set. The class label is gender, encoded as a self-reported binary attribute in the Facebook-100 distribution (Lim et al., 2021); LI is near zero because friendship communities are not gender-segregated, but the topology itself encodes community structure. We note that conclusions about aggregator behavior on these datasets are tied to this specific demographic prediction task: the topological signal that drives the sum-wins regime may not transfer to other tasks on dense social networks, and the use of self-reported binary gender labels in Facebook-100 carries known limitations and biases (expanded, with non-demographic alternatives, in the Broader Impact Statement). We hypothesized that sum aggregation captures this structural community signal through degree-weighted accumulation that mean aggregation discards. To test this, we trained GIN-Sum and GIN-Mean on SBM graphs at a 9×5 grid of (target h, target mean degree) settings with random within-block class assignment, isolating the role of mean degree at LI ≈ 0; full results are in Appendix B. Mean aggregation won across the entire grid we tested, with the gap becoming *more* negative (mean wins more) as degree increases at low h — the wrong direction relative to the LINKX observations. Sum aggregation won in 0 of 15 cells in the highest-degree, low-h corner. The SBM ablation provides evidence against uniform mean degree as the sole cause within the degree range we tested ($\bar{d} \leq 30$); we cannot rule it out at LINKX-comparable degrees ($\bar{d} = 48$–70) where the comparison becomes degenerate. Our SBM is also simpler than real friendship networks: it lacks heavy-tailed degrees and multi-scale communities. Appendix F rules out node features as the cause: replacing one-hot demographic attributes with Gaussian noise leaves the sum-wins gap intact and amplifies it by 50–106% on the three evaluable datasets ($p = 0.002$ in each). The responsible property is therefore topological; which topological property triggers the regime remains an open question. To close this high-degree gap, a degree-corrected SBM reaching $\bar{d} \in \{50, 60, 70\}$ (Appendix B) likewise produces no sum-wins regime: GIN-Sum wins in 8 of 15 high-degree cells, a chance-level proportion (binomial $p = 0.50$) with no degree trend ($\rho(\bar{d}, \text{gap}) = +0.14$), in contrast to the consistent sum-wins on all five LINKX graphs.

The spectral gap separates LINKX from other low-LI graphs. While no scalar statistic in the homophily family predicts the LINKX regime, we find that one structural statistic outside that family cleanly separates it from the other low-LI datasets where mean aggregation succeeds. We computed clustering coefficient, modularity, degree assortativity, degree skewness, and the algebraic connectivity λ_2 (second eigenvalue of the normalized Laplacian) for all 24 benchmarks (Appendix H). Global Spearman correlation with the gap is uninformative for λ_2 ($\rho = +0.05$, n.s.), because high-LI datasets are already explained by LI and dilute the correlation; λ_2 is a *regime-specific* discriminator, not a global predictor. Within the low-LI regime (LI < 0.05), the five LINKX datasets have $\lambda_2 \in [0.078, 0.178]$, whereas all six low-LI non-LINKX datasets have $\lambda_2 \leq 0.067$: the two groups are perfectly rank-separated. The resulting Mann–Whitney $p = 0.0022$ is the combinatorial floor of the test at this sample size ($1/\binom{11}{5} = 0.00216$) and therefore certifies complete separation rather than a small probability of chance; it remains below 0.05 after Bonferroni correction for the five structural statistics screened ($5 \times 0.00216 = 0.011$). Because λ_2 was selected post hoc as the best of these five discriminators, we do not treat this single test as confirmatory — the load-bearing evidence that the LINKX regime is structural is its *independent replication* under GCN (Section 4.6, Appendix J) and its *strengthening* under BatchNorm (Appendix I). Modularity shows the converse: LINKX graphs have markedly lower modularity (mean $Q = 0.33$) than the comparison group (mean $Q = 0.58$, Mann–Whitney $p = 0.014$), consistent with their being dense friendship networks whose communities are not class-segregated. The LINKX graphs are expander-like (high λ_2, low Q); the low-LI datasets where mean aggregation wins have strong community bottlenecks (near-zero λ_2). We hypothesize that in expander-like graphs mean aggregation pulls node representations toward a global mean, discarding the structural signal that unnormalized sum preserves. Tolokers ($\lambda_2 = 0.067$, $\bar{d} = 88.3$) sits just below the LINKX λ_2 band yet mean aggregation wins, so λ_2 is the strongest single discriminator we identify but not a perfect threshold rule; a multivariate characterization remains open. This elevates the LINKX regime from "unexplained by any statistic we tested" to "separated by a structural statistic outside the homophily family," a concrete and testable refinement.

The effect is localized to the one-hop neighborhood. To localize the effect by aggregation depth, we re-ran GIN-Sum and GIN-Mean at depths 1–4 on the LINKX datasets (Appendix K). At depth 1, GIN-Sum wins on every evaluable LINKX dataset (gaps +0.013 to +0.236); at depth ≥ 2 the gap collapses or reverses on three of four. The sum-wins effect is therefore carried by the immediate one-hop neighborhood and is diluted by additional aggregation hops — consistent with the expander-mixing hypothesis, since in a high-λ_2 graph each extra mean-aggregation hop mixes node representations toward the global mean faster than sum.

The LINKX surprise is robust to extended training. To rule out the alternative explanation that the LINKX surprise is a training-stability artifact, we re-ran the four smaller LINKX datasets with 1000 epochs and patience 200 (versus 300/50 in the main grid). The GIN-Sum vs. GIN-Mean gap held or grew larger under extended training on every dataset (Appendix C). The mechanism is consistent: GIN-Sum's best validation epoch ranges from 208 to 589, while GIN-Mean's plateaus at 65–81 across all four datasets and never recovers. Penn94, the largest LINKX graph (41,554 nodes, 2.7M edges), exceeded available GPU memory under full-batch longer training; we report only its default-300-epoch result (+7.1% gap, $p = 0.002$).

4.4 Three training regimes

In characterizing per-dataset results we observe three distinct training regimes that interact with aggregator selection.

Stable-learning (21 of 24 datasets). All GIN variants train past epoch 20 with non-trivial accuracy above the majority-class baseline. The aggregator gap is well-defined and interpretable.

Sum-saves-it (Roman-empire only). GIN-Mean and GIN-Max collapse to majority-class accuracy; only GIN-Sum extracts graph signal, consistent with Xu et al.'s expressiveness result. This single-dataset observation is isolated to avoid conflating it with stable-learning datasets.

All-collapse (Amazon-ratings, Cornell). All GIN variants converge to majority-class predictions. These are null results for the aggregator question and are excluded from rule-fitting analyses.

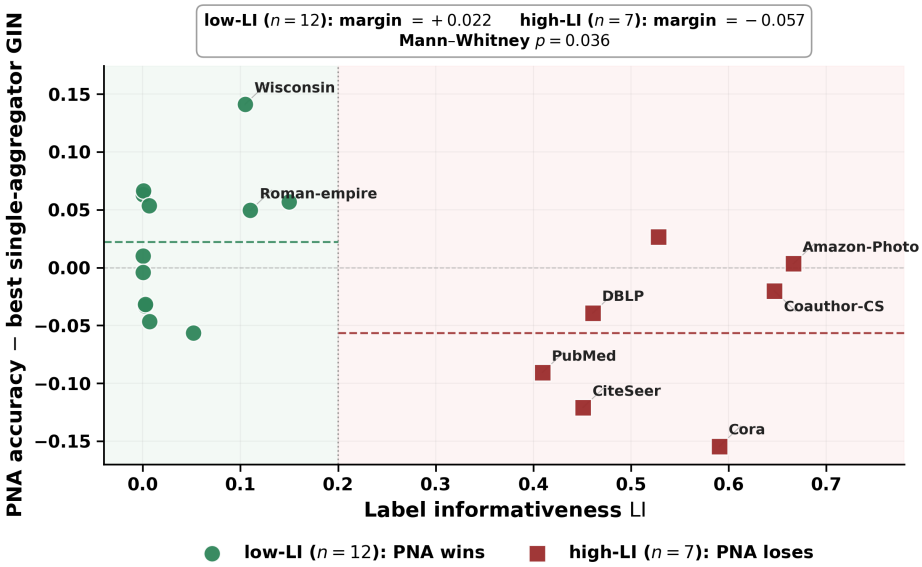

Figure 2: PNA (Corso et al., 2020) accuracy minus the best single-aggregator GIN variant, plotted against label informativeness. PNA wins on low-LI graphs (mean margin +0.022) and loses on high-LI graphs (mean margin −0.057, Mann–Whitney $p = 0.036$); removing the three citation networks leaves the high-LI comparison non-significant ($p = 0.446$), so the effect is concentrated there. PNA has no coverage of the LINKX regime due to memory constraints.

Regime classification rule. Let a^* be the majority-class baseline, $\bar{a}_v$ the mean accuracy of variant v, and σ_v its standard deviation. *All-collapse*: $\max_v \bar{a}_v - a^* < 0.005$ and $\max_v \sigma_v < 0.005$, or all variants produce identical per-seed accuracies. *Sum-saves-it*: $\bar{a}_{\text{Sum}} - a^* > 0.02$ and $\max_{v \neq \text{Sum}} \bar{a}_v - a^* < 0.01$, meaning mean and max both fall below baseline. *Stable-learning*: all other datasets. Cornell is all-collapse (identical per-seed accuracies, gap = 0); Amazon-Computers is stable-learning because GIN-Mean's low accuracy (0.373) is aggregator-specific rather than graph-level. Under this rule, Cornell and Amazon-ratings are all-collapse, Roman-empire is sum-saves-it, and the remaining 21 datasets are stable-learning.

Threshold stability. To check that regime assignments do not depend on the exact threshold values, we re-ran the classifier across 12 different threshold settings. 21 of 24 datasets received the same assignment in every setting; details are in Appendix D.

4.5 PNA is not uniformly better than the best single aggregator

PNA (Corso et al., 2020) combines multiple aggregators with learnable degree scalers and is often presented as a default-strong choice. We compare it to the best single-aggregator GIN per dataset.

PNA results are available for 21 of the 24 datasets; the three exceptions are Coauthor-Physics, Cornell5, and Penn94, where PNA exceeded available GPU memory at hidden dimension 64.[2] We further exclude the two all-collapse datasets (Amazon-ratings, Cornell) for which aggregator comparison is a null result by definition (Section 4.4), leaving $n = 19$ datasets in the analysis.

PNA wins on 9 of 19 datasets but with mean margin near zero (−0.007). The pattern is more revealing when split by LI: on low-LI graphs (LI < 0.2, $n = 12$), PNA wins by mean margin +0.022; on high-LI graphs (LI ≥ 0.2, $n = 7$), PNA loses by mean margin −0.057.[3] A Mann–Whitney U test on the margin distributions yields $p = 0.036$. Figure 2 shows the per-dataset margins against LI. The strongest losses are on the standard citation networks: Cora (−0.155), CiteSeer (−0.121), and PubMed (−0.091).

[2]PNA exceeded GPU memory at both hidden dimension 64 and 32 for these three datasets due to its degree-scaler computation; the analysis therefore proceeds with $n = 19$ datasets.

[3]We use the LI ≥ 0.2 cut here; because no dataset in our suite has LI $\in [0.2, 0.4)$, this partitions the datasets identically to the LI ≥ 0.4 cut used in Section 4.2 and Appendix G, and the choice of threshold within that gap is immaterial.

The loss is concentrated on citation networks specifically: removing Cora, CiteSeer, and PubMed leaves the Mann–Whitney test on the remaining four high-LI datasets non-significant ($p = 0.446$), so PNA's machinery imposes a meaningful cost precisely where sum aggregation is strongly preferred, while results on other high-LI graphs are mixed. These conclusions hold under 2-layer, hidden-dim-64, full-batch training. PNA's higher memory use meant we could not test it on Cornell5 and Penn94 — two of the five LINKX graphs where the sum-wins anomaly is strongest. The PNA analysis has no coverage of the most interesting regime; reducing hidden dim to 32 does not resolve the OOM (Appendix E). The PNA conclusions are therefore strongest on the citation networks where PNA loses badly, and effectively absent on the LINKX regime where the comparison would matter most. As a partial probe, neighbor-sampled mini-batch PNA (Appendix E) does reach four of the five LINKX graphs and loses to single-aggregator GIN on all four (mean margin -0.144), echoing the citation-network result; mini-batch approximation, however, makes these numbers not directly comparable to the full-batch grid.

4.6 Cross-architecture generalization

GraphSAGE replication (Appendix A) confirms the aggregator gap is partially graph-determined: GIN and GraphSAGE agree on sign for 18 of 24 datasets ($\rho = 0.75$, $p = 3 \times 10^{-5}$). However, the LI predictor does not transfer ($\rho_{\text{SAGE}} = 0.32$, n.s.). Disagreements concentrate on high-LI citation networks (Cora, CiteSeer); disabling GraphSAGE's self-loop pathway widens rather than closes the gap (Table 3), so the mechanism remains open.

GCN: the LINKX effect is not GIN-specific. We additionally tested a custom GCN variant that replaces the $D^{-1/2}AD^{-1/2}$ normalization with unnormalized sum aggregation, keeping all other architecture and training choices fixed (Appendix J). Unlike the GraphSAGE result, the LI rule *partially transfers* to GCN: on the 16 stable-learning non-LINKX datasets, $\rho(\text{LI}, \text{GCN-Sum} - \text{GCN-Mean gap}) = +0.574$ ($p = 0.016$) — significant but weaker than the GIN value of 0.885. More importantly, the LINKX sum-wins anomaly *replicates and amplifies* in GCN: GCN-Sum outperforms GCN-Mean on all four evaluable LINKX datasets, with gaps of +7.5 to +20.8% versus GIN's +5.0 to +10.3%, amplifying on three of the four (e.g. Amherst41 +9.3% → +17.2%; JohnsHopkins55 +10.3% → +20.8%; Reed98 is the smallest at +5.0% → +7.5%). The LINKX regime is therefore a property of degree-normalized aggregation on these graphs, not an artifact of the GIN architecture. One boundary disagreement is worth noting: on Tolokers, GIN favors mean (-0.057) while GCN favors sum ($+0.085$), consistent with Tolokers sitting at the λ_2 boundary identified in Section 4.3.

5 Discussion

Benchmark composition as the hidden variable. The LI rule achieves 88% LOO ($\rho = 0.885$) on 16 stable-learning non-LINKX datasets; adding LINKX drops ρ to 0.51 and LOO to majority baseline. Legacy benchmarks contain no datasets at LI ≈ 0 with high mean degree — Facebook-100 fills this gap. The dependency is methodological, not numerical: the LINKX surprise strengthens under extended training (Section 4.3), and the rule does not transfer to GraphSAGE ($\rho_{\text{SAGE}} = 0.32$, n.s.) so all conclusions are GIN-specific unless replicated. Setting aside the architectural scope, there is a second and separate failure: even within GIN, the LI rule breaks down on a specific graph family that legacy benchmarks never include. Dense friendship networks at near-zero LI occupy a region of graph-statistic space that no standard benchmark suite covers. The most obvious scalar explanation — high mean degree — is not supported within our tested range ($\bar{d} \leq 30$) (Appendix B), and node features are ruled out by a randomization experiment showing the gap grows when features are replaced with Gaussian noise (Appendix F). The cause is topological but unidentified. Finding what actually causes the LINKX regime would turn this empirical anomaly into a usable design rule. Degree-corrected SBMs or LFR benchmarks, which better capture heavy-tailed degrees and multi-scale community structure, are natural next steps for testing candidate explanations.

Activation scale versus structural expressiveness. A BatchNorm ablation (Appendix I) separates the two mechanisms confounded in the no-normalization GIN. The three extreme high-LI gaps — Coauthor-CS (+51.9%), Amazon-Computers (+45.6%), Amazon-Photo (+56.6%) — shrink by 75–96% when activation scales are equalized (to +1.9%, +6.3%, +14.4% respectively), so those particular margins are substantially

inflated by activation-scale dynamics on dense graphs; the structural component survives but is small. The LINKX effect behaves oppositely: under BatchNorm the LINKX gaps *grow* (Amherst41 +9.3% → +30.2%, Cornell5 +7.5% → +16.3%, Reed98 +5.0% → +10.5%), with GIN-BN-Mean collapsing to chance accuracy on Amherst41 across all seeds. Equalizing activation scale therefore does not remove the LINKX regime — it strengthens it — confirming the LINKX effect is structural rather than a scale artifact, while the largest high-LI margins are partly scale-driven.

Limitations and implications. Transfer of the LI rule to attention-based or heterophily-specialized architectures remains open. The hyperparameter sweep does not vary normalization, residual connections, or activation; Penn94 exceeded GPU memory under longer training, so training-stability evidence relies on the four smaller LINKX datasets.

For practitioners using GIN-family models: on graphs where LI ≥ 0.4, GIN-Sum outperforms PNA and is the better default; on near-zero LI graphs, run both GIN-Sum and GIN-Mean and compare per-seed. Whether this guidance extends to GraphSAGE, GAT, or other architectures requires separate validation. For benchmark designers, LI is strictly better than homophily but leaves a documented failure mode (Facebook-100); a statistic that captures community structure independently of class labels would close this gap.

Future experimental directions. Several follow-up directions remain. A degree-corrected SBM with power-law degrees does not reproduce the LINKX regime (Appendix B), and the spectral-gap separation (Section 4.3) is suggestive but not a perfect rule (Tolokers is a boundary counterexample); an LFR or degree-corrected SBM constructed to match LINKX-scale λ_2 *and* community structure simultaneously is the natural next synthetic testbed. Our preliminary attempt at a learnable temperature-scaled sum aggregator (sum divided by $\bar{d}^{\alpha}$) was inconclusive: α initialized at the sum solution did not move under gradient descent, indicating a flat local landscape rather than evidence for or against the moderated-sum hypothesis (Appendix I). A constrained or annealed parameterization of α is required to test this hypothesis properly and remains future work. Transfer of the LI rule to attention-based and heterophily-specialized architectures, and a model-parallel PNA implementation able to reach Penn94, remain open.

6 Conclusion

Our central finding is that the LINKX Facebook-100 family constitutes a regime where neither edge homophily nor label informativeness predicts GIN aggregator preference. Node features are ruled out (Appendix F), and the anomaly is more precisely *degree-normalised aggregation fails* than *sum wins* (Appendix G). The responsible property is topological: the spectral gap separates the LINKX graphs from every other low-LI dataset (Mann–Whitney $p = 0.002$) and the effect is localized to the one-hop neighborhood, though no single scalar threshold yet predicts the regime perfectly (Tolokers is a boundary counterexample). Label informativeness predicts the GIN-Sum vs. GIN-Mean gap with $\rho = 0.885$ and 88% LOO accuracy on 16 stable-learning datasets, yet the same rule collapses to majority baseline on LINKX, where four datasets at LI ≈ 0 exhibit +7% to +13% sum-wins gaps that strengthen under tenfold-extended training. These findings are established for GIN; the partial transfer to GraphSAGE ($\rho = 0.32$) suggests the LI rule is architecture-dependent. Identifying the structural property behind the LINKX regime would extend Platonov et al.'s critique of homophily-based diagnostics, and would give adaptive aggregation methods a concrete benchmark target.

Broader Impact Statement

The LINKX datasets central to our analysis use a self-reported binary gender attribute as the classification target. We use this label only because it defines the established benchmark and enables comparison with prior LINKX work; we do not treat binary gender as an adequate representation of gender identity, and models trained on it should not be used to infer gender for real individuals. Because Appendix F shows the effect is topology-driven and independent of node features, the same structural question can be studied with non-demographic or synthetic targets (e.g. class year or a synthetic community label), which we recommend for future work and which our released code supports.

Reproducibility Statement

Code and notebooks are available at `https://github.com/nehasharmacs/aggregator-rule-supplement/blob/main/README.md`. `00_quickstart_analysis.ipynb` reproduces all main-text figures and statistics in under five minutes on CPU; `01`–`05` re-run the training grid on a single GPU; `08_new_experiments.ipynb` regenerates supplementary results (Appendices H–B) from cached outputs. Per-seed results, split indices, sweep configurations, and structural statistics are included.

References

Sami Abu-El-Haija, Bryan Perozzi, Amol Kapoor, Nazanin Alipourfard, Kristina Lerman, Hrayr Harutyunyan, Greg Ver Steeg, and Aram Galstyan. MixHop: Higher-order graph convolutional architectures via sparsified neighborhood mixing. In *International Conference on Machine Learning (ICML)*, 2019.

Wei-Lin Chiang, Xuanqing Liu, Si Si, Yang Li, Samy Bengio, and Cho-Jui Hsieh. Cluster-gcn: An efficient algorithm for training deep and large graph convolutional networks. In *KDD*, 2019.

Eli Chien, Jianhao Peng, Pan Li, and Olgica Milenkovic. Adaptive universal generalized PageRank graph neural network. In *International Conference on Learning Representations (ICLR)*, 2021.

Gabriele Corso, Luca Cavalleri, Dominique Beaini, Pietro Liò, and Petar Veličković. Principal neighbourhood aggregation for graph nets. In *Advances in Neural Information Processing Systems (NeurIPS)*, 2020.

Mounir Ghogho. Revisiting neighborhood aggregation in graph neural networks for node classification using statistical signal processing. pp. 1–5, 2025. doi: 10.1109/ICASSP49660.2025.10888683.

William L. Hamilton, Rex Ying, and Jure Leskovec. Inductive representation learning on large graphs. In *Advances in Neural Information Processing Systems (NeurIPS)*, 2017.

Asela Hevapathige, Asiri Wijesinghe, and Ahad N Zehmakan. Beyond fixed depth: Adaptive graph neural networks for node classification under varying homophily. In *Proceedings of the AAAI Conference on Artificial Intelligence*, volume 40, pp. 21717–21725, 2026.

Weihua Hu, Matthias Fey, Marinka Zitnik, Yuxiao Dong, Hongyu Ren, Bowen Liu, Michele Catasta, and Jure Leskovec. Open graph benchmark: Datasets for machine learning on graphs. In *Advances in Neural Information Processing Systems (NeurIPS)*, 2020.

Thomas N. Kipf and Max Welling. Semi-supervised classification with graph convolutional networks. In *International Conference on Learning Representations (ICLR)*, 2017.

Derek Lim, Felix Hohne, Xiuyu Li, Sijia Linda Huang, Vaishnavi Gupta, Omkar Bhalerao, and Ser Nam Lim. Large scale learning on non-homophilous graphs: New benchmarks and strong simple methods. In *Advances in Neural Information Processing Systems (NeurIPS)*, 2021.

Sitao Luan, Chenqing Hua, Qincheng Lu, Jiaqi Zhu, Mingde Zhao, Shuyuan Zhang, Xiao-Wen Chang, and Doina Precup. Revisiting heterophily for graph neural networks. In *Advances in Neural Information Processing Systems (NeurIPS)*, 2022.

Sitao Luan, Chenqing Hua, Minkai Xu, Qincheng Lu, Jiaqi Zhu, Xiao-Wen Chang, Jie Fu, Jure Leskovec, and Doina Precup. When do graph neural networks help with node classification? investigating the impact of homophily principle on node distinguishability. In *Advances in Neural Information Processing Systems (NeurIPS)*, 2023.

Yuankai Luo, Lei Shi, and Xiao-Ming Wu. Classic gnns are strong baselines: Reassessing gnns for node classification. In *Advances in Neural Information Processing Systems (NeurIPS)*, 2024.

Yao Ma, Xiaorui Liu, Neil Shah, and Jiliang Tang. Is homophily a necessity for graph neural networks? In *International Conference on Learning Representations (ICLR)*, 2022.

Sunil Kumar Maurya, Xin Liu, and Tsuyoshi Murata. Simplifying approach to node classification in graph neural networks. *Journal of Computational Science*, 62:101695, 2022. ISSN 1877-7503. doi: https://doi.org/10.1016/j.jocs.2022.101695. URL `https://www.sciencedirect.com/science/article/pii/S1877750322000990`.

Hongbin Pei, Bingzhe Wei, Kevin Chen-Chuan Chang, Yu Lei, and Bo Yang. Geom-gcn: Geometric graph convolutional networks. In *International Conference on Learning Representations (ICLR)*, 2020.

Oleg Platonov, Denis Kuznedelev, Michael Diskin, Artem Babenko, and Liudmila Prokhorenkova. A critical look at the evaluation of gnns under heterophily: Are we really making progress? In *International Conference on Learning Representations (ICLR)*, 2023.

Oleksandr Shchur, Maximilian Mumme, Aleksandar Bojchevski, and Stephan Günnemann. Pitfalls of graph neural network evaluation. In *Relational Representation Learning Workshop, NeurIPS*, 2018.

Jie Tang, Jimeng Sun, Chi Wang, and Zi Yang. Social influence analysis in large-scale networks. In *KDD*, 2009.

Petar Veličković, Guillem Cucurull, Arantxa Casanova, Adriana Romero, Pietro Liò, and Yoshua Bengio. Graph attention networks. In *International Conference on Learning Representations (ICLR)*, 2018.

Keyulu Xu, Weihua Hu, Jure Leskovec, and Stefanie Jegelka. How powerful are graph neural networks? In *International Conference on Learning Representations (ICLR)*, 2019.

Zhilin Yang, William W. Cohen, and Ruslan Salakhutdinov. Revisiting semi-supervised learning with graph embeddings. In *International Conference on Machine Learning (ICML)*, 2016.

Jiong Zhu, Yujun Yan, Lingxiao Zhao, Mark Heimann, Leman Akoglu, and Danai Koutra. Beyond homophily in graph neural networks: Current limitations and effective designs. In *Advances in Neural Information Processing Systems (NeurIPS)*, 2020.

A Cross-Architecture Replication: Full Results

We trained GraphSAGE-Sum, GraphSAGE-Mean, and GraphSAGE-Max on all 24 benchmarks under the identical training protocol used for GIN. Figure 3 shows the per-dataset GIN gap versus GraphSAGE gap. We hypothesized that GraphSAGE's separate self-loop transformation provides the count-preserving signal that sum contributes in GIN, reducing the marginal benefit of sum on high-LI graphs. To test this, we retrained GraphSAGE-Sum and GraphSAGE-Mean with `root_weight=False` (disabling the self-loop transformation in PyG's `SAGEConv`) on Cora, CiteSeer, and PubMed — the three high-LI datasets where standard GraphSAGE-Sum loses to GraphSAGE-Mean.

Table 3: GraphSAGE-Sum minus GraphSAGE-Mean accuracy gap with and without the self-loop transformation (`root_weight=False`). Standard SAGE column uses the 10-seed main grid; no-root SAGE column uses 5 seeds. Paired Wilcoxon p in parentheses; differences in p between columns partly reflect seed counts (Wilcoxon floor at $n = 5$ is $p \approx 0.062$; at $n = 10$ is $p = 0.002$).

Dataset	Standard SAGE	No-root SAGE
Cora	-0.024 ($p = 0.005$)	-0.068 ($p = 0.042$)
CiteSeer	-0.070 ($p = 0.005$)	-0.083 ($p = 0.043$)
PubMed	$+0.012$ ($p = 0.012$)	$+0.035$ ($p = 0.043$)

Removing the self-loop does not recover the GIN-like Sum-wins pattern on Cora or CiteSeer; on both datasets Mean wins by a *larger* margin without root-weight (-6.8% and -8.3% respectively, versus -2.4% and -7.0% in the standard model). PubMed shifts slightly toward Sum ($+1.2\% \rightarrow +3.5\%$), consistent with the hypothesis, but PubMed already exhibited a Sum-wins gap in the standard model. The ablation does not support the self-loop pathway as the mechanism responsible for the GIN–GraphSAGE disagreement on high-LI citation graphs. Identifying the actual mechanism is left to future work.

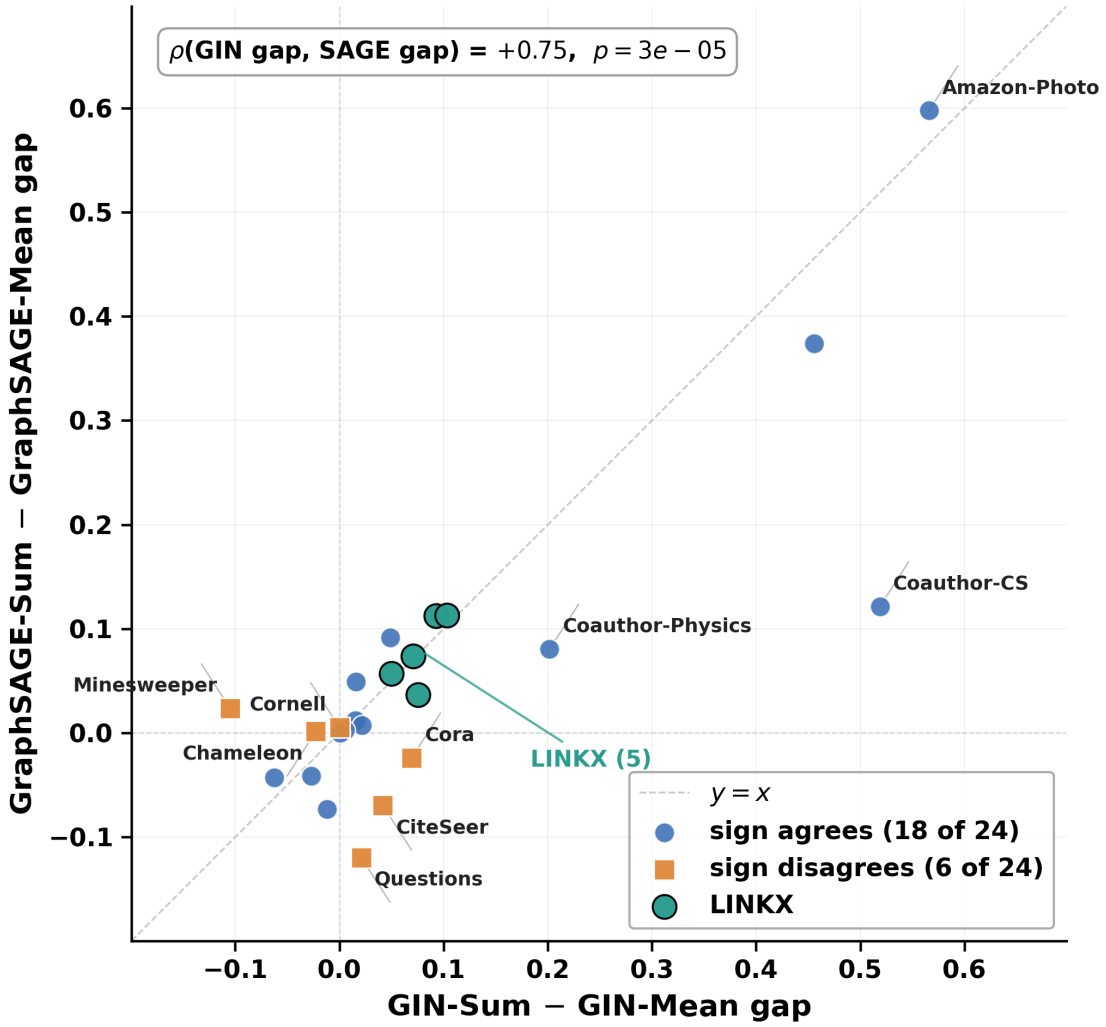

Figure 3: Per-dataset GIN-Sum minus GIN-Mean gap (x-axis) versus GraphSAGE-Sum minus GraphSAGE-Mean gap (y-axis). Spearman $\rho = 0.75$ ($p = 3 \times 10^{-5}$); 18 of 24 datasets agree on aggregator preference. Disagreements concentrate on the high-LI citation networks.

B SBM Validation Results

To test whether high mean degree alone explains the LINKX-family sum-wins regime, we trained GIN-Sum and GIN-Mean on stochastic block model graphs across a 9×5 grid of target homophily $h \in \{0.1, 0.2, \ldots, 0.9\}$ and target mean degree $\bar{d} \in \{3, 9.75, 16.5, 23.25, 30\}$. Class labels were assigned uniformly at random within each block, driving label informativeness LI to approximately zero by construction. Each cell uses 5 random initializations.

Figure 4 shows the per-cell GIN-Sum minus GIN-Mean accuracy gap. The hypothesis that high mean degree triggers a sum-wins regime at LI ≈ 0 is not supported within the tested range: Spearman $\rho(\bar{d}, \text{gap}) = +0.12$ ($p = 0.42$) across the full grid, and at low h (where LI is closest to zero by construction) the mean gap is -0.16 at the highest tested degree — mean aggregation wins. Sum aggregation wins in 0 of 15 cells in the high-degree, low-h corner, in direct contrast to the four LINKX Facebook-100 datasets where GIN-Sum wins by 7–13%.

Tested-range scope. Our SBM grid maxes out at mean degree $\bar{d} = 30$; the LINKX Facebook-100 graphs have median degree 48–70, the highest in our benchmark suite. We did not extend the SBM grid to LINKX-comparable degrees because at $\bar{d} \geq 60$ on graphs of the size we generated, GIN-Mean approached zero validation loss within the first few epochs and the comparison became degenerate. The negative finding therefore reads as "high mean degree in the range we tested ($\bar{d} \leq 30$) does not produce a sum-wins regime at LI ≈ 0" rather than a global ruling-out across all degrees. Even with this scope caveat, the trend visible in Figure 4 is the wrong direction: at fixed low h, the gap becomes *more* negative (mean wins more) as degree increases, with no sign reversal in sight. Extrapolating the visible trend, even at $\bar{d} = 60$ the SBM would predict a mean-wins regime, in contradiction with the LINKX observations.

This negative result indicates that the LINKX surprise reported in Section 4.3 is not reducible to mean degree. Real friendship networks differ from our SBM construction in several ways: their degree distributions are heavy-tailed rather than within-block uniform, their community structure is multi-scale, and their node features (one-hot demographic attributes in the LINKX distribution) carry information correlated with the class label even when neighborhoods themselves do not. Degree-corrected stochastic block models or LFR benchmarks would capture the heavy-tailed degree distributions and multi-scale communities of real friendship networks more faithfully than the homogeneous SBM we used; extending the negative result to these models is a natural next step. We report the present negative result as evidence that the LINKX regime is genuinely outside the scope of current degree-based and homophily-based graph statistics, and constitutes a discovered open problem rather than an explained one.

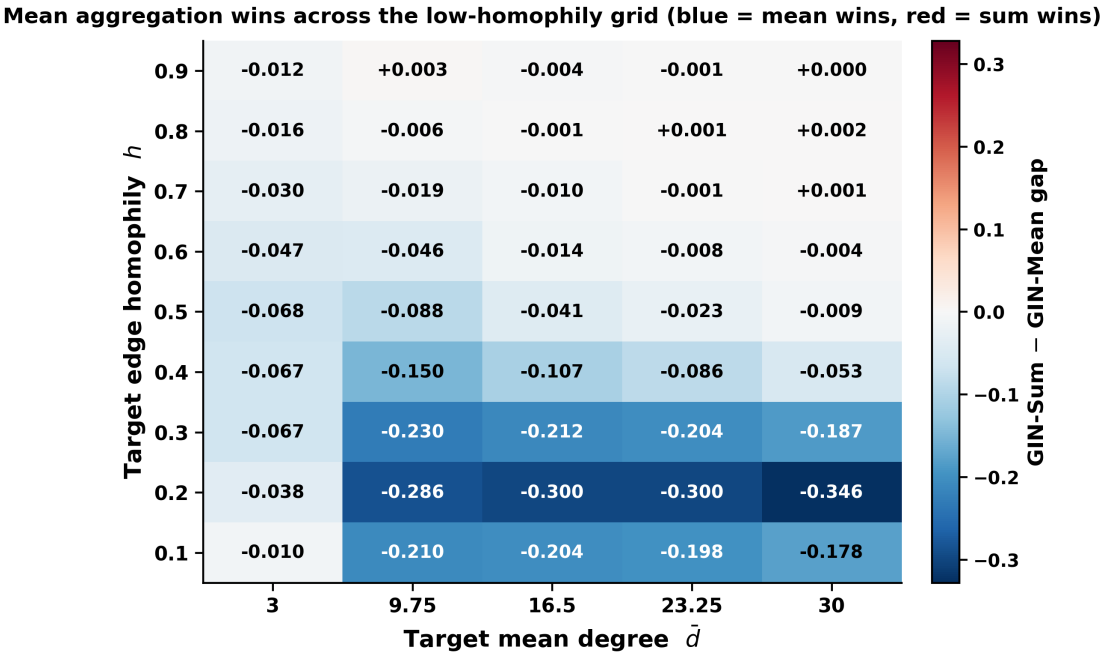

Figure 4: GIN-Sum minus GIN-Mean accuracy gap on stochastic block model graphs across a 9×5 grid of target homophily $h \in \{0.1, \ldots, 0.9\}$ and target mean degree $\bar{d} \in \{3, 9.75, 16.5, 23.25, 30\}$. Each cell averages 5 random initializations. Mean aggregation wins (negative gap, blue) across all low-h cells and in every cell at the degrees relevant to the LINKX comparison; the few near-zero positive cells at high h ($\leq +0.003$) are negligible. The gap does not become positive at the highest tested degree in any low-h cell, and the visible trend at low h is in the wrong direction (gap becomes more negative as degree increases).

Degree-corrected SBM at LINKX-scale degrees. To address the tested-range scope caveat above, we repeated the ablation with a degree-corrected SBM whose degree sequence follows a power law ($\tau = 2.5$), extending the grid to mean degrees $\bar{d} \in \{50, 60, 70\}$ that match the LINKX range, with block-correlated labels controlled to keep LI ≈ 0. Across the 5×6 grid (5 seeds per cell), GIN-Sum wins in 8 of 15 high-degree cells

($\bar{d} \geq 50$), a proportion indistinguishable from chance (one-sided binomial $p = 0.50$), and there is no degree trend ($\rho(\bar{d}, \text{gap}) = +0.14$, $p = 0.45$). Combining the homogeneous SBM above with this degree-corrected extension rules out both uniform and heavy-tailed degree heterogeneity as standalone triggers of the LINKX regime, across the full degree range that LINKX occupies.

C LINKX Longer-Training Detail

Per-dataset gap evolution under 1000-epoch, patience-200 training (3 seeds per cell), versus the 300-epoch default-grid result: Reed98 +5.0% → +5.9%; Amherst41 +9.3% → +12.8%; Cornell5 +7.5% → +10.3%; JohnsHopkins55 +10.3% → +10.1%. On every dataset the gap held or grew under extended training, ruling out training-stability as the source of the LINKX surprise.

D Regime Classification Threshold Sensitivity

We re-ran the regime classifier over a 4×3 grid of perturbed threshold triples (collapse_eps $\in \{0.001, 0.005, 0.01, 0.02\}$; sum-saves-it thresholds scaled proportionally), yielding 12 settings in total. Of the 24 datasets, 21 retain their regime assignment across all 12 settings. The three boundary cases are: Amazon-ratings (reclassified to stable-learning only when collapse_eps is reduced to 0.001, five times below the reference value); Roman-empire (reclassified to stable-learning only when the sum-saves-it margin threshold is raised to 0.05, 2.5 times the reference 0.02); and Wisconsin (reclassified to sum-saves-it at tighter thresholds, where its +0.016 gap barely crosses the margin criterion). The core assignments that drive the paper's conclusions — Cornell and Amazon-ratings as all-collapse, Roman-empire as the sole sum-saves-it dataset — are stable across the entire perturbation grid.

E PNA Extended Analysis: OOM Datasets

Section 4.5 excludes Coauthor-Physics, Cornell5, and Penn94 because PNA exceeded GPU memory at hidden dimension 64. To close this gap, we attempted to re-run PNA at hidden dimension 32 on all three datasets (identical training protocol, 3 seeds each). All three datasets triggered `OutOfMemoryError` even at hidden dimension 32, due to PNA's degree-scaler computation scaling with graph size independently of hidden dimension.

The n=12/7 split from Section 4.5 therefore cannot be extended. The three excluded datasets span both LI regimes: Cornell5 (LI = 0.01) and Penn94 (LI = 0.00) would join the Low-LI group; Coauthor-Physics (LI = 0.72) would join the High-LI group. The direction of any bias introduced by their exclusion is therefore mixed: Low-LI loses two dense LINKX graphs where sum wins strongly (likely making PNA look relatively better in that group), and High-LI loses a high-degree coauthorship graph (direction unknown). The Mann–Whitney result of $p = 0.036$ should be interpreted with this coverage gap in mind, as stated in Section 4.5.

A CPU-based mini-batch implementation of PNA or model parallelism would be required to evaluate these datasets; we leave this to future work.

Mini-batch PNA on LINKX. Using neighbor-sampled mini-batch training (`NeighborLoader`, 2-hop fan-out 10×10, batch size 1024), we obtained PNA results on four of the five LINKX datasets (Penn94 still exceeded host memory during full-graph evaluation). Mini-batch PNA loses to the best single-aggregator GIN on all four: Reed98 (−0.076), Amherst41 (−0.169), JohnsHopkins55 (−0.175), Cornell5 (−0.158), mean margin −0.144. PNA's multi-aggregator machinery does not recover the structural signal that single-aggregator GIN-Sum extracts on dense friendship networks, consistent with the high-LI citation-network finding in Section 4.5. Mini-batch sampling introduces approximation error relative to full-batch training, so these numbers are not directly comparable to the main grid and are reported only to fill the LINKX coverage gap.

F LINKX Feature Randomization

Section 4.3 leaves open whether the LINKX sum-wins anomaly is driven by node features or graph topology. The LINKX node features are one-hot demographic attributes; if they carry community signal invisible to label informativeness, removing them should collapse the gap. To test this, we replaced the node features in all five LINKX datasets with i.i.d. Gaussian noise of identical dimension ($x_v \sim \mathcal{N}(0, I)$), holding the graph topology, labels, and train/val/test masks fixed. All other training details are identical to the main grid (Section 3).

Penn94 and Cornell5 triggered `OutOfMemoryError` under this configuration, consistent with their behaviour in the main grid and in Appendix E; we report results for the three datasets that completed (Reed98, Amherst41, JohnsHopkins55), covering the full range of original gap magnitudes in the LINKX family.

Table 4: GIN-Sum minus GIN-Mean accuracy gap on LINKX datasets with original vs. randomized node features (10 seeds each; paired Wilcoxon p on random-feature runs). Penn94 and Cornell5 OOM under both conditions.

Dataset	Original gap	Random-feature gap	Δ	p
Reed98	+0.050	+0.077	+0.027	0.002
Amherst41	+0.093	+0.190	+0.098	0.002
JohnsHopkins55	+0.103	+0.155	+0.052	0.002
Penn94	+0.071	OOM		
Cornell5	+0.075	OOM		

The sum-wins gap does not collapse under feature randomization; on all three evaluable datasets it *grows* (by +54%, +106%, and +50% respectively), and remains significant at $p = 0.002$ in each case. This rules out the hypothesis that one-hot demographic node features carry community signal that drives the anomaly. The effect is **topology-driven**: the dense friendship graph structure itself causes GIN-Sum to outperform GIN-Mean at near-zero label informativeness, independently of what node features are supplied.

This result sharpens the open problem identified in Section 4.3: the responsible structural property is a topological one, not a feature-distribution one. The gap growing under randomization is consistent with original features partially *suppressing* the topological signal in GIN-Mean (e.g. if demographic features provide a shortcut that reduces reliance on neighborhood structure), but we do not test this interpretation further. Degree-corrected SBMs or LFR benchmarks, which replicate heavy-tailed degree distributions and multi-scale community structure without informative node features, are the natural next synthetic testbed for isolating the responsible topological property.

G GIN-Max Aggregation: Full Analysis

The main paper focuses on GIN-Sum vs. GIN-Mean because that comparison is theoretically grounded in Xu et al. (2019)'s expressiveness results. GIN-Max results are present in the main grid but not systematically analyzed. We report the full three-way comparison here, as it reveals structure that qualifies several of the paper's findings.

Max wins more often than Mean. Across the 22 stable-learning datasets (excluding Cornell and Amazon-ratings, Section 4.4), GIN-Sum achieves the highest mean accuracy on 13 datasets, GIN-Max on 8, and GIN-Mean on 1 (Actor). Mean aggregation is almost never the best single aggregator; the practically relevant competition is between Sum and Max.

LI does not predict the Sum–Max gap. The Spearman correlation between label informativeness and the GIN-Sum minus GIN-Max accuracy gap is $\rho = +0.196$ ($p = 0.38$) across all 22 datasets, and $\rho = +0.385$ ($p = 0.13$) on the 17 non-LINKX datasets. Neither is significant. By contrast, LI predicts the Sum–Mean gap at $\rho = 0.885$ ($p < 0.001$) on the same non-LINKX set (Section 4.2). LI is therefore specifically diagnostic for the Sum–Mean choice; it carries no reliable information about whether Sum or Max is preferable.

Max does not collapse on high-LI graphs. On the seven high-LI datasets (LI ≥ 0.4) where GIN-Mean collapses dramatically, GIN-Max tracks GIN-Sum closely (Table 5). The mean accuracy of GIN-Max on these datasets is 0.783, versus 0.796 for GIN-Sum and 0.534 for GIN-Mean. The exception is Amazon-Computers, where both GIN-Max (0.373) and GIN-Mean (0.373) collapse while GIN-Sum reaches 0.829; this suggests that on some high-degree co-purchase graphs the count-preserving property of sum aggregation is structurally necessary, not merely advantageous. The general pattern is that Mean's degree-normalization discards discriminative signal on high-LI graphs, while Max's elementwise selection largely preserves it.

Table 5: GIN-Sum, GIN-Mean, and GIN-Max accuracy on high-LI datasets (LI ≥ 0.4). Max tracks Sum closely on most datasets where Mean collapses. Best per row in **bold**.

Dataset	LI	GIN-Sum	GIN-Mean	GIN-Max
PubMed	0.41	0.774	0.758	**0.780**
CiteSeer	0.45	**0.609**	0.567	0.600
DBLP	0.46	0.845	0.824	**0.848**
Amazon-Computers	0.53	**0.829**	0.373	0.373
Cora	0.59	**0.755**	0.686	0.730
Coauthor-CS	0.65	**0.925**	0.406	0.920
Amazon-Photo	0.67	**0.899**	0.333	0.896
Coauthor-Physics	0.72	0.962	0.760	**0.963**

LINKX regime: Mean loses, Sum and Max are competitive. On the five LINKX Facebook-100 datasets, GIN-Sum wins on four (Penn94, Amherst41, Cornell5, JohnsHopkins55) and GIN-Max wins on one (Reed98, by 0.005); GIN-Mean never wins (Table 6). The LINKX anomaly is more precisely characterised as *Mean loses* than *Sum wins*: both aggregators that avoid degree normalisation (Sum and Max) outperform the normalised Mean on dense friendship networks. This further constrains the topological explanation established in Appendix F: the responsible property specifically impairs degree-normalised aggregation, not neighbourhood aggregation in general.

Table 6: Three-way GIN comparison on LINKX Facebook-100 datasets. GIN-Mean never wins; both Sum and Max outperform it.

Dataset	GIN-Sum	GIN-Mean	GIN-Max	Best
Penn94	**0.807**	0.736	0.772	Sum
Reed98	0.625	0.576	**0.630**	Max
Amherst41	**0.775**	0.683	0.771	Sum
Cornell5	**0.802**	0.726	0.766	Sum
JohnsHopkins55	**0.783**	0.679	0.752	Sum

Low-LI regime: Max wins more than Mean. On the six low-LI non-LINKX datasets (LI < 0.1), GIN-Max wins on four (Minesweeper, Squirrel, Tolokers, Chameleon), GIN-Mean on one (Actor), and GIN-Sum on one (Questions). The "mean-wins" characterisation of the low-LI regime in the main paper is a simplification: Max is the more reliable aggregator on these datasets. The practical implication for GIN-family practitioners is that GIN-Max should be included in per-seed comparisons on low-LI non-LINKX graphs, not only GIN-Sum and GIN-Mean.

H Structural Fingerprinting: Full Results

To identify what distinguishes the LINKX regime from other low-LI datasets, we computed five label-independent structural statistics for all 24 benchmarks: global clustering coefficient, greedy-modularity Q, degree assortativity, degree-distribution skewness, and the algebraic connectivity λ_2 (second-smallest eigenvalue of the symmetric normalized Laplacian). For disconnected graphs λ_2 is computed on the largest

connected component; only JohnsHopkins55 was materially disconnected (11 components, 5157 of 5180 nodes in the LCC), and we report its LCC value ($\lambda_2 = 0.126$).

Sensitivity to graph preprocessing. We computed λ_2 on the undirected graph without adding self-loops; for the single materially disconnected dataset (JohnsHopkins55) we used the largest connected component, as noted above, and every other graph has a single dominant component covering $> 99\%$ of nodes. The choice between the symmetric normalized Laplacian $L_{\text{sym}} = I - D^{-1/2}AD^{-1/2}$ and the random-walk normalized Laplacian $L_{\text{rw}} = I - D^{-1}A$ does not change any reported value: the two are similar matrices ($L_{\text{rw}} = D^{-1/2}L_{\text{sym}}D^{1/2}$) and hence share the same spectrum, so λ_2 is identical under either convention. Adding self-loops before computing λ_2 would shift the individual values; we did not do so, but because the LINKX and non-LINKX low-LI groups are separated by roughly an order of magnitude ($\lambda_2 \in [0.078, 0.178]$ versus ≤ 0.067), the group-level rank separation reported in Table 7 is expected to be robust to this convention.

Global Spearman correlations with the GIN-Sum minus GIN-Mean gap across all 24 datasets are weak for every structural statistic (all $|\rho| < 0.25$, none significant after the LI/h predictors already in the main text), because the high-LI datasets are explained by LI and dominate the global ranking. The informative test is within the low-LI regime. Restricting to the 11 datasets with LI < 0.05 and splitting into the five LINKX graphs versus the six non-LINKX low-LI graphs (Squirrel, Actor, Amazon-ratings, Minesweeper, Tolokers, Questions):

Table 7: Structural statistics within the low-LI regime (LI < 0.05): $n = 5$ LINKX datasets (Penn94, Reed98, Amherst41, Cornell5, JohnsHopkins55) versus $n = 6$ non-LINKX low-LI datasets (Squirrel, Actor, Amazon-ratings, Minesweeper, Tolokers, Questions). p is a one-sided Mann–Whitney U test of the indicated direction. Spectral gap and modularity each separate the two groups; clustering, assortativity, and skew do not.

Statistic	LINKX mean	non-LINKX mean	Mann–Whitney p
Spectral gap λ_2	0.131	0.019	0.0022 (LINKX greater)
Modularity Q	0.334	0.580	0.014 (LINKX lower)
Clustering	0.27	0.33	0.18 (n.s.)
Assortativity	+0.04	−0.04	0.40 (n.s.)
Degree skew	5.3	11.8	0.31 (n.s.)

The five LINKX datasets occupy $\lambda_2 \in [0.078, 0.178]$ while all six low-LI non-LINKX datasets have $\lambda_2 \leq 0.067$; the only near-overlap is Cornell5 (0.078) versus Tolokers (0.067). Spectral gap is thus the strongest single structural discriminator of the LINKX regime, but the Cornell5/Tolokers proximity and the fact that Tolokers' aggregator preference matches the low-LI (mean) side under GIN show that no single threshold perfectly separates the groups; a multivariate (λ_2, Q) rule is the natural next step. The spectral-gap separation is consistent with an expander-mixing account: LINKX graphs are well-connected expanders (high λ_2, low Q), and the low-LI datasets where mean wins have strong community bottlenecks (near-zero λ_2). Concretely, mean aggregation corresponds to the random-walk propagation operator $D^{-1}A$ (similar to the symmetric $D^{-1/2}AD^{-1/2}$ and therefore sharing its spectrum), whose largest eigenvalue is 1 — the degree-weighted global-average direction — and whose remaining eigenvalues are separated from it by the spectral gap λ_2. The component of the node representations orthogonal to that global direction is contracted relative to it by a factor of $1 - \lambda_2$ per aggregation hop, so a large gap (an expander) drives representations toward the global average within one or two hops. Unnormalized sum instead applies A, which has no such normalization and preserves degree-scaled magnitude, retaining the local discriminative signal that mean discards. This account predicts the effect should be strongest at a single hop and dilute with depth — exactly the depth-1 localization reported in Appendix K. We present this as motivating intuition consistent with our observations, not a tight bound: λ_2 is a between-regime discriminator rather than a closed-form rule, and Tolokers is a boundary counterexample. We emphasize that λ_2 separates the LINKX family from other low-LI datasets at the group level but does *not* rank-order the gap within the LINKX family (e.g. Reed98 has the highest $\lambda_2 = 0.178$ yet nearly the smallest gap, +0.050; Penn94 at $\lambda_2 = 0.155$ has gap +0.071). The spectral gap is therefore a between-regime discriminator, not a within-regime effect-size predictor — consistent with our claim that it isolates the regime but does not constitute a closed-form rule.

I BatchNorm Ablation

The main-text GIN uses no normalization, leaving a confound between aggregator expressivity and activation-scale dynamics on dense graphs (noted in Section 3). To separate the two, we added BatchNorm after the first linear layer of each GIN-MLP and re-ran GIN-BN-Sum and GIN-BN-Mean (5 seeds) on the high-LI datasets where the sum-wins gap is largest and on the LINKX datasets. We exclude Cora and CiteSeer: their public-split training sets (140/120 nodes) are too small for stable BatchNorm statistics, and accuracy collapsed to 0.11–0.48 for both aggregators, making the comparison uninterpretable. Penn94 exceeded GPU memory as in the main grid. We note that the structural conclusion below – that LINKX gaps *grow* under BatchNorm – is established on the LINKX datasets alone and does not depend on the high-LI exclusions; the Cora/CiteSeer removal affects only finding (i) (the high-LI scale-artifact result), where those two datasets are not among the three extreme-gap cases under discussion.

Table 8: GIN-Sum minus GIN-Mean gap, original (no-norm, main grid) versus with BatchNorm. Extreme high-LI gaps shrink sharply; LINKX gaps grow.

Dataset	Original gap	BatchNorm gap	Change
Coauthor-CS	+0.519	+0.019	−96%
Amazon-Computers	+0.456	+0.063	−86%
Amazon-Photo	+0.566	+0.144	−75%
Reed98	+0.050	+0.105	+110%
Amherst41	+0.093	+0.302	+225%
Cornell5	+0.075	+0.163	+117%

Two findings emerge. (i) The three extreme high-LI margins shrink by 75–96% once activation scales are equalized, so those particular numbers are substantially inflated by scale dynamics on high-degree graphs; a positive structural component remains but is small (+0.02–+0.14). (ii) The LINKX gaps *grow* under BatchNorm, with GIN-BN-Mean collapsing to chance accuracy on Amherst41 (mean 0.50, all five seeds stopping at epoch 1) while GIN-BN-Sum reaches 0.77–0.81. Equalizing activation scale therefore strengthens rather than removes the LINKX effect, corroborating the conclusion (Appendix F) that the LINKX regime is structural. We also tested a learnable degree-scaled sum aggregator ($\text{sum}/\bar{d}^{\alpha}$, α learnable, initialized to 0); α did not move from its initialization on any dataset, including low-LI datasets where mean aggregation is preferred, indicating a flat gradient at the initialization rather than a learned preference. We therefore report this sub-experiment as inconclusive and draw no conclusion from α.

J GCN Cross-Architecture Replication

We implemented a GCN variant in which the symmetric normalization $D^{-1/2}AD^{-1/2}$ is replaced by unnormalized sum aggregation (self-loops retained in both variants), holding the 2-layer, hidden-64, dropout-0.5, Adam training protocol identical to the main grid. GCN-Sum versus GCN-Mean was run for 10 seeds on all 24 datasets.

On the 16 stable-learning non-LINKX datasets, the LI rule partially transfers: $\rho(\text{LI}, \text{GCN gap}) = +0.574$ ($p = 0.016$), significant but weaker than the GIN value of 0.885. Cross-model agreement is moderate: $\rho(\text{GIN gap}, \text{GCN gap}) = +0.668$ ($p = 0.001$). The LINKX sum-wins anomaly replicates and amplifies in GCN:

The LINKX regime is therefore a property of degree-normalized aggregation on these graphs, not specific to the GIN architecture. We interpret the larger GCN gaps cautiously: GCN-Sum removes the $D^{-1/2}AD^{-1/2}$ normalization entirely, whereas GIN-Sum retains the $(1+\varepsilon)\mathbf{x}$ self-term, so the amplification is consistent with the structural account but could also reflect GCN-Sum being a more degenerate unnormalized operator than GIN-Sum. The directional agreement across architectures is the robust claim; the magnitude difference should not be over-interpreted.

Table 9: LINKX sum-vs-mean gap under GIN versus the GCN variant. The effect is larger in GCN on every evaluable LINKX dataset.

Dataset	GIN gap	GCN gap
Reed98	+0.050	+0.075
Amherst41	+0.093	+0.172
Cornell5	+0.075	+0.143
JohnsHopkins55	+0.103	+0.208

K Depth Sensitivity on LINKX

We re-ran GIN-Sum and GIN-Mean at depths 1, 2, 3, 4 (5 seeds) on the five LINKX datasets to localize the sum-wins effect by aggregation hop. Penn94 exceeded memory at depth ≥ 3; we report the four smaller datasets.

Table 10: GIN-Sum minus GIN-Mean gap by depth on LINKX. The advantage is concentrated at depth 1 and dilutes or reverses with more hops.

Dataset	$d = 1$	$d = 2$	$d = 3$	$d = 4$
Reed98	+0.013	−0.017	−0.012	−0.013
Amherst41	+0.236	−0.024	−0.070	+0.004
Cornell5	+0.105	−0.068	−0.055	−0.042
JohnsHopkins55	+0.093	+0.071	−0.059	−0.036

GIN-Sum wins at depth 1 on all four datasets; by depth ≥ 2 the gap has collapsed or reversed on three of four. The sum-wins signal is therefore carried by the one-hop neighborhood and is diluted by additional aggregation hops. This is consistent with the expander-mixing account (Appendix H): in a high-λ_2 graph, each additional mean-aggregation hop mixes node representations toward the global mean faster than sum, erasing the local structural signal that sum preserves at one hop. We note the claim rests on four datasets (one of which, JohnsHopkins55, retains a positive gap at depth 2), so we present it as consistent with the expander-mixing account rather than as an independently established depth mechanism.